SYNCHRONOUS CONTROL OF A STATIC AC INDUCTION MOTOR DRIVE

A.B.Plunkett J.D.D'Atre T.A.Lipo
General Electric Co.
Schenectady,N.Y.

Presented at the 1977
IEEE/IAS Annual Mtg.
Los Angeles CA, Oct.2-6 1977

Summary

Conventional methods of controlling an induction motor utilize regulation of stator current and motor slip frequency in order to maintain system stability. This control strategy requires a shaft speed feedback and fast response current regulation. An alternative method of controlling an induction motor is presented which achieves the necessary system stabilization by controlling only the motor frequency. The control inherently regulates the motor torque angle by properly adjusting the phase of the converter firing signals. By synchronizing the inverter firing pulses to the motor back EMF possible adverse inverter operating modes are avoided. The concept of synchronous control eliminates the preprogrammed functional relations previously required and allows the control to adapt to any desired motor flux level. Any desired outer regulating loop can be incorporated to form a fast response, wide range AC drive system.

Introduction

During recent years the development of static AC drives has opened up new fields of application for AC machines. These new applications have, in turn, necessitated the development of fast response, high accuracy regulating systems. One regulating system which has prompted considerable attention is the current regulated induction motor drive. The basic configuration of such a drive is shown in Fig. 1. In this system AC or DC power is converted to variable amplitude DC power by means of a phase controlled AC/DC rectifier or DC/DC chopper. The power is then converted to AC form by means of a DC/AC converter. A filter is inserted in the DC link so as to smooth the ripple currents inherent in rectifier or chopper operation. Alternatively, the AC to AC conversion could be accomplished in one step by use of a cycloconverter.

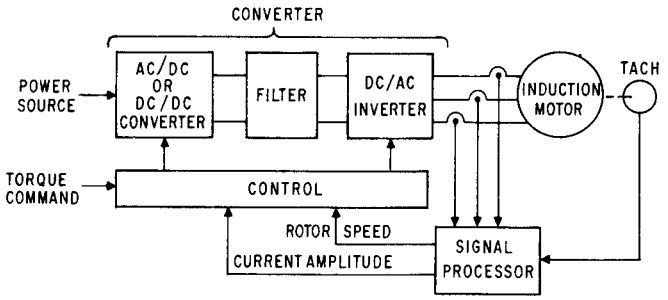

Fig. 1 Static AC drive with current and speed feedback.

In order to realize practical operation of both motor and converter, stabilizing feedback must often be used to maintain normal motor flux and current levels.[1] Conventional control methods realize this stabilization by dynamic control of the motor current amplitude. Such strategy requires that the converter respond over the entire operating speed-torque range since system stability could be lost should the converter (rectifier, chopper or cycloconverter) be phased fully on. The constraint severely limits the speed range over which such systems can be practically applied since operation in the "field weakening" or constant horsepower mode becomes difficult. In addition to current regulation, a function of current is used to set the motor slip frequency which together with a motor speed feedback signal sets the inverter firing frequency.[2,3] This functional relationship between link current and slip frequency is established to maintain, approximately, a constant flux in the motor as a function of load. The motor electrical slip frequency can also be calculated from terminal voltage and current.[4] However, accurate knowledge of motor parameters is required. Since motor parameters change with stator current, air gap flux, rotor frequency and temperature these regulation schemes are inherently difficult to operate over a wide range of speed and load. Stability can also be maintained by controlling power factor[5] but parameter changes again deteriorate performance.

In this paper an alternative method of control is presented. The scheme utilizes the inverter frequency as the necessary system stabilizing control while the current amplitude merely adjusts the motor steady-state flux level. The stabilization is achieved by regulating the phase angle between motor current and motor flux. This approach causes the inverter firing pulses to synchronize to the motor counter-EMF and is the dual of the voltage fed induction motor wherein additional current is inherently provided to align the motor counter-EMF to the inverter.[6]

The concept of synchronous control evolved from a desire to synchronize current flow in the inverter with respect to motor counter-EMF. It appears that an inverter with current regulation functions very much as a phase-controlled rectifier operating in the inverting mode. The firing angle of the inverter must be synchroized with respect to the motor voltage (or internal flux) in order to smoothly control power flow. Lack of synchronization results in an effect similar to the oscillation of a synchronous motor subjected to a sudden load change in which the rotor of the machine oscillates with respect to synchronous speed. Damping of rotor swings in a synchronous motor is obtained from short-circuited rotor windings which generate transient voltages which in turn draw transient currents from the power supply to damp the oscillation. In the case of an induction motor supplied by a current source a similar oscillating effect exists. However, the required damping current does not inherently flow from the power supply. By synchronizing the converter to the motor counter-EMF such hunting-type instabilities can be eliminated.

In addition to stability problems caused by hunting, difficulties are also introduced by converter commutation. Commutation introduces a time delay between the firing of a converter thyristor and the instant of actual current transfer in the motor lines. Ripple currents introduce additional random delays in the commutation time. Unless properly treated, these delays can cause difficulties in inverter firing and in subsequent loss of control. The concept of synchronous control allows the effects of variable inverter commutation delay to be attenuated by the gain within the regulation loop. Synchronous control also offers the possibility of tachometerless operation. The expense and mechanical problems associated with a tachometer can be eliminated.

General Concepts

The conventional d-q axes equivalent circuit of a squirrel-cage induction motor expressed in a reference frame fixed in the stator[7] is given in Fig. 2. The quantities shown are the standard motor equivalent circuit parameters defined in the usual manner. The variables ψ_{mq}, ψ_{md}, ψ'_{qr}, and ψ'_{dr} correspond to the q- and d-axis air gap and rotor flux linkages respectively. These flux quantities carry units of voltage, are equal to the corresponding flux linkages λ times ω_b, the base angular frequency and are defined by

$$\psi_{mq} = \omega_b L_m (i_{qs} + i'_{qr}) \quad (1)$$

$$\psi_{md} = \omega_b L_m (i_{ds} + i'_{dr}) \quad (2)$$

$$\psi'_{qr} = \omega_b [(L_m + L'_{\ell r}) i'_{qr} + L_m i_{qs}] \quad (3)$$

$$\psi'_{dr} = \omega_b [(L_m + L'_{\ell r}) i'_{dr} + L_m i_{ds}] \quad (4)$$

In general, the superscript 's' is usually affixed to the d-q variables to signify the stator reference frame but the practice is omitted here for convenience. The quantities $(\omega_r/\omega_b)\psi'_{qr}$ and $(\omega_r/\omega_b)\psi'_{dr}$ can be considered as equivalent to the generated counter EMF of the motor and are cross-coupled between the d- and q- axes.

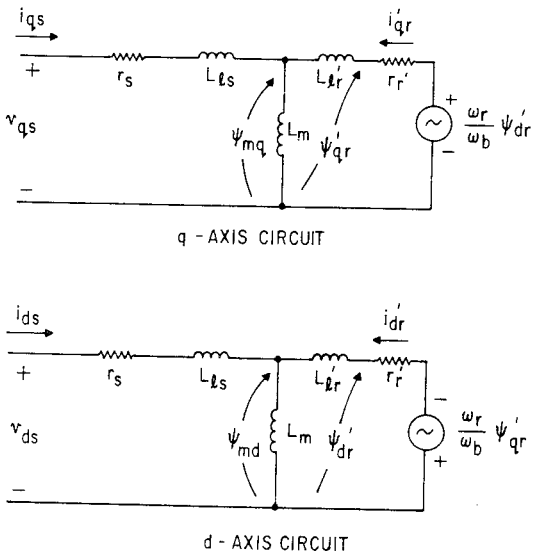

Fig. 2 Induction motor d-q equivalent circuit in the stationary reference frame.

Figures 3 and 4 are vector diagrams portraying the q- and d- axis quantities as two components of a vector in order to show the interrelations which exist between variables. In particular, Fig. 3 shows the change in angular position of the motor current vectors as a function of load at rated speed using the air gap flux linkage vector as reference. The parameters of an experimental system given the Appendix were used wherein 750 ft lb corresponds approximately to rated load. At no load, the flux and current vector are in phase and 90° out of phase with the terminal voltage vector. When the motor load increases, rotor current must be developed which in turn requires a counteracting component of stator current.

It can be observed that the stator voltage vector $\hat{v}_s$ does not significantly change position with load so that the frequency (or phase) of a voltage source need not vary with changes in load. The voltage source also offers an inherent stabilizing action by supplying damping current so that the motor is able to rapidly align to any new operating condition without assistance from the inverter. On the other hand, it can be noted that the stator current magnitude and angle change rapidly with load. The angular relation between current and motor flux now depends on the inverter firing and must be artificially provided by the control when a current source is employed. In addition, sufficient damping must be provided by the control for good transient behavior since the damping currents which normally flow are not inherently present.

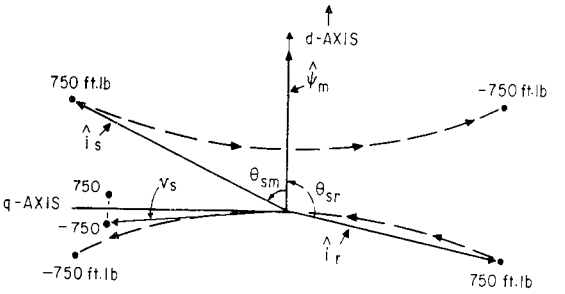

Fig. 3 Loci of voltage, current and flux linkage vectors with load at rated frequency.

A similar realignment effect occurs with voltage source inverters at low speeds except it is now the terminal voltage vector that must be changed with respect to the flux vector. Fig. 4 shows a vector diagram illustrating a transition through zero speed while maintaining torque constant. It should be noted that the current and flux linkage vectors remain relatively fixed while the terminal voltage vector varies widely in angle and magnitude with speed. The firing pulses of a voltage inverter source must now be aligned at the correct phase with respect to the motor flux such that a change from braking to motoring can occur without a transient. An angle control is now required when operating from a voltage source. Note, however, that with a current source the corresponding flux-current vector alignment is achieved without difficulty.

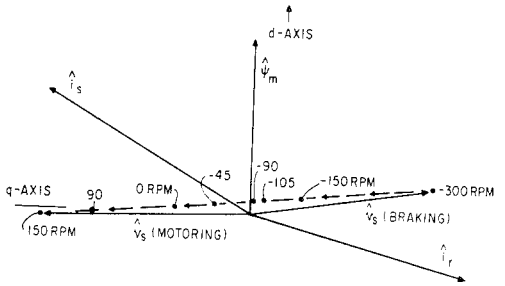

Fig. 4 Loci of voltage, current and flux linkage vectors during speed reversal. Torque maintained constant.

Calculation of Torque Angle

In general, the calculation of torque angle necessitates sensing motor electrical variables since this quantity cannot be directly measured as with a synchronous machine. One alternative is to measure motor line current and terminal voltage and back-calculate the flux angular position from the per phase induction motor equivalent circuit. Unfortunately, motor parameters vary from motor to motor, with temperature, and with load conditions so that such compensation may become

inaccurate, particularly at low speeds where resistance drop becomes the largest portion of motor voltage. A preferred method is to sense the air gap flux directly.[8,9] Since the air gap flux is the result of both stator and rotor currents the actual rotor circuit operating conditions are sensed and the inaccuracies involved in termainal measurements can be eliminated.

It can be shown that when stator current and air gap flux linkages are written as vectors having d- and q- components then the electromagnetic torque can be expressed

$$\hat{T}_e = (\frac{3}{2})(\frac{P}{2})\frac{1}{\omega_b}\hat{i}_s \times \hat{\psi}_m \tag{5}$$

where P is the number of motor poles and 'x' denotes the cross product between the current and flux linkage vectors. Equation 5 can be written alternatively as

$$T_e = (\frac{3}{2})(\frac{P}{2})\frac{1}{\omega_b}|\hat{i}_s||\hat{\psi}_m|\sin\theta_{sm} \tag{6}$$

where θ_{sm} is the angle between $\hat{i}_s$ and $\hat{\psi}_m$. Thus, the torque angle can be computed from the equation.

$$\sin\theta_{sm} = \frac{4\omega_b T_e}{3P|\hat{i}_s||\hat{\psi}_m|} \tag{7}$$

In general, Eq. 7 is the most straightforward means for computing torque angle. However, other forms for the torque equation exist which yield other possible flux-current relationships. It can be shown that Eqs. 8-10 are alternative expressions for instantaneous electromagnetic torque[10]

$$\hat{T}_e = (\frac{3}{2})(\frac{P}{2})\frac{1}{\omega_b}\hat{\psi}_m \times \hat{i}_r \tag{8}$$

$$\hat{T}_e = (\frac{3}{2})(\frac{P}{2})\frac{1}{\omega_b}\hat{\psi}_s \times \hat{i}_r \tag{9}$$

$$\hat{T}_e = (\frac{3}{2})(\frac{P}{2})\frac{1}{\omega_b}\hat{i}_s \times \hat{\psi}_r \tag{10}$$

where $\hat{\psi}_s$ denotes the total stator flux linkage vector and $\hat{i}_r$ is the rotor current vector. Unfortunately the rotor current cannot be monitored directly so that Eqs. 8 and 9 are difficult to implement. However, from Eqs. 1-4 the rotor and air gap flux linkages can be written

$$\hat{\psi}_r = x'_{\ell r}\hat{i}_r + \hat{\psi}_m \tag{11}$$

$$\hat{\psi}_m = x_m(\hat{i}_s + \hat{i}_r) \tag{12}$$

where $x'_{\ell r} = \omega_b L'_{\ell r}$ and $x_m = \omega_b L_m$. Upon algebraically eliminating $\hat{i}_r$, Eq. 11 can be written

$$\hat{\psi}_r = \frac{x'_r}{x_m}\hat{\psi}_m - x'_{\ell r}\hat{i}_s \tag{13}$$

where $x'_r = x'_{\ell r} + x_m$. Hence, the rotor flux linkage vector can be mechanized from the air gap flux linkages and stator current. The angle θ_{sr} between $\hat{i}_s$ and $\hat{\psi}_r$ corresponding to Eq. 10 can also be viewed as a torque angle. The angle θ_{sr} is defined by

$$\sin\theta_{sr} = \frac{4\omega_b T_e}{3P|\hat{i}_s||\hat{\psi}_r|} \tag{14}$$

and $\hat{\psi}_r$ is derived from Eq. 13.

The quantities $\sin\theta_{sm}$ and $\sin\theta_{sr}$ are plotted as functions of slip frequency in Fig. 5. Again the system parameters given in the Appendix were used. It can be noted that the quantity $\sin\theta_{sm}$ is a double valued function of torque when slip frequency increases from zero to breakdown. Since the angle control is located within a torque regulation loop, difficulties can be anticipated by this double-valued behavior. It can be noted that the angle between stator current and rotor flux is not double-valued but reaches a maximum of 90° when the slip frequency approaches breakdown. However, the angle change is very small at high slips indicating low gain and consequent poor regulation.

One practical modification of this angle measurement technique is to basically provide a corrective signal to ensure that a monotonic relationship is maintained between torque and angle. Although Eq. 13 is a vector relationship it is interesting to consider the approximate relationship

$$|\hat{\psi}_r| \simeq \frac{x'_r}{x_m}|\hat{\psi}_m| - x'_{\ell r}|\hat{i}_s| \tag{15}$$

Equation 14 becomes

$$(\sin\theta)_{eq.} = \frac{4\omega_b T_e}{3P[\frac{x'_r}{x_m}|\hat{\psi}_m| - x'_{\ell r}|\hat{i}_s|]|\hat{i}_s|} \tag{16}$$

The equivalent angle quantity $(\sin\theta)_{eq.}$ is also plotted in Fig. 5. Note that this modified variable takes on values greater than unity and thus does not strictly correspond to an actual angle. Nonetheless, the quantity increases monotonically over the entire operating region and thereby suggests a feasible variable for regulation.

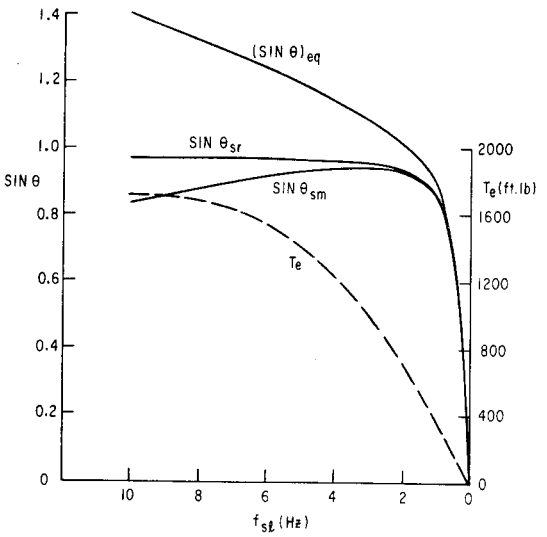

Fig. 5 Torque and torque angle as a function of slip.

Transient Behavior of Synchronous Control

Although it has been demonstrated that a modified value of torque angle has desirable steady-state properties, a detailed dynamic analysis is required in order to verify that the proposed angle regulation scheme is feasible. One analysis technique which has proven ideally suited to this task is the computation of the relevant induction motor transfer functions.[11] As part of this technique the d-q equations which express dynamic behavior of the inverter-motor system are defined, linearized for small changes about an operating

point and recast in state variable form.[3] The relavant transfer function input is defined and the output is identified in terms of the state variables. The equations are then transformed to phase-variable canonical form wherein the desired transfer function can be obtained by inspection. Having obtained the desired transfer function, any of the usual control design techniques can be employed such as Bode plot, root-locus plot, Nichols chart, etc.

It has already been mentioned that when the DC voltage source is active, the required system stabilization can be achieved by utilizing the DC link. One desirable control scheme which has been reported previously[9] is shown in Fig. 6. With this method, the air gap flux magnitude and air gap torque are sensed. The DC voltage source is used to regulate the amplitude of the air gap flux and an inner current loop is provided to eliminate the time constant associated with the DC link inductor. In addition, slip frequency is adjusted to regulate the torque to the desired level.

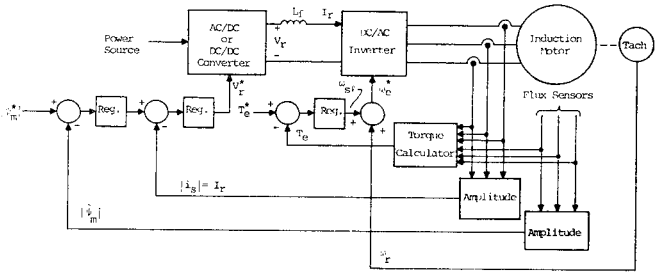

Fig. 6 Control scheme employing flux amplitude and torque regulation.

In Fig. 7 the flux loop has been disabled and the DC link current loop has been closed through a simple gain G_i. That is

$$V_r = G_i(I_r^* - I_r) \qquad (17)$$

where the asterisk denotes the commanded value of link current which is assumed constant. Figure 7 shows the migration of the poles and zeros of the frequency loop transfer function between slip angular frequency and air gap torque, $(\Delta T_e/\Delta\omega_{s\ell})$, as the gain G_i is increased in the DC link current regulator. The operating point considered is at rated frequency, rated terminal volts/Hz. and a load of 750 ft.lb. The system parameters in the Appendix were again used. Note that although the system poles are in the right half plane for zero gain, the poles move into the left half plane with only a modest amount of feedback gain when the current regulator is in operation. Control of slip frequency is not required for stabilization. In Fig. 7 the effects of rotor speed changes have been neglected. Although rotor speed changes slightly modify the results of Fig. 7 the inertia will be assumed infinitely large throughout this study.

In Fig. 8 the behavior of the same transfer function is investigated. However, this time the current regulator is out of service indicating that the DC voltage source is fixed. This condition corresponds to operation at high speeds in which the AC/DC rectifier or DC/DC chopper is phased full on (fully conducting). Figure 8 shows the location of the poles and zeros of $\Delta T_e/\Delta\omega_{s\ell}$ for a range of load points. Note that the system becomes unstable for loads above about 150 ft.lb. Moreover the complex conjugate poles in the right half plane are accompanied by a pair of zeros indicating that overall stability is not possible regardless of the feedback compensator used between the output ΔT_e and input $\Delta\omega_{s\ell}$. This behavior clearly points to the need for an improved control scheme during high speed operation.

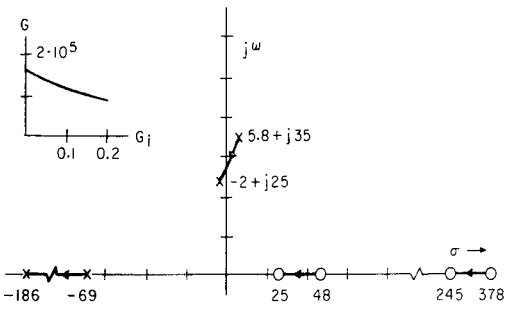

Fig. 7 Poles(x), zeros(0), and gain(G) of transfer function $\Delta T_e/\Delta\omega_{s\ell}$ for increasing link current regulator gain G_i. Initial point G_i=0, final point G_i=0.2. Operating condition 50 Hz., 210V. 750 ft.lb.

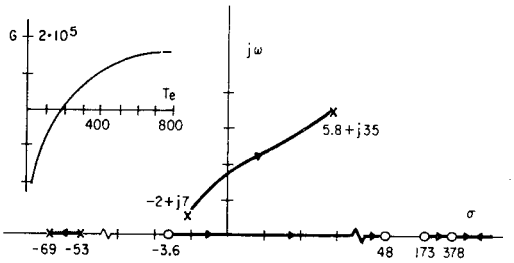

Fig. 8 Poles(x), zeros(0), and gain(G) of transfer function $\Delta T_e/\Delta\omega_{s\ell}$ with constant DC link voltage. Effect of increasing load torque with rated terminal voltage and frequency. Initial point T_e= 25, final point T_e=750 ft.lb.

In Fig. 9 the sine of the angle between stator current and air gap flux linkage, $\sin\theta_{sm}$ has been implemented by means of Eq. 7. The poles and zeros of $\Delta(\sin\theta_{sm})/\Delta\omega_{s\ell}$ are plotted over the same range of operating conditions as in Fig. 8. Since the transfer function pole locations are independent of input and output the poles again enter the right half plane at 150 ft.lb. as load is increased. In this case the zeros originate at -2 and -52 at no load. The zeros move together, break off the real axis, and then return at a load of 500 ft.lb. Up to this point the zeros migrate only in the left half plane indicating that stabilization remains feasible. However, as load continues to increase, one of the zeros moves to the right and finally enters the right half plane beyond 1000 ft.lb. The point at which this zero changes sign corresponds to the inflection point of the plot of $\sin\theta_{sm}$ vs. $f_{s\ell}$ in Fig. 5. In general, one of the right half plane poles will be attracted to this zero as feedback gain is increased so that stabilizing feedback compensation appears impractical if not impossible.

Figure 10 shows the pole-zero locations when the quantity $\sin\theta_{sr}$ is measured rather than $\sin\theta_{sm}$. It can be noted that the zeros are better behaved and never enter the right half plane. However, the system gain changes dramatically with load. Although it is possible to compensate with a feedback gain which increases inversly with load, such a technique is difficult to mechanize because practical considerations such as noise and sampling effects begin to affect performance.

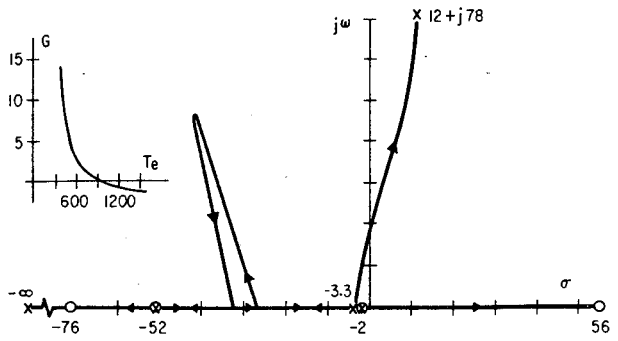

Fig. 9 Poles(x), zeros(0), and gain(G) of transfer function $\Delta\sin\theta_{sm}/\Delta\omega_{s\ell}$ with constant DC link voltage. Effect of increasing load torque with rated terminal voltage and frequency. Initial point T_e=0 (no-load), final point T_e=1675 ft. lb. (breakdown).

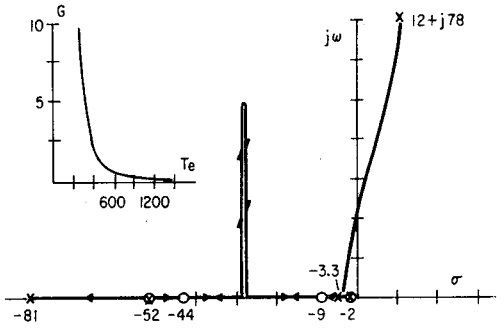

Fig. 10 Poles(x), zeros(0), and DC gain(G) of transfer function $\Delta\sin\theta_{sr}/\Delta\omega_{s\ell}$ with constant DC link voltage. Effect of increasing load torque with rated terminal voltage and frequency. Initial point T_e=0, final point T_e=1675 ft.lb.

In Fig. 11 the modified angle derived from Eqs. 15 and 16 is considered as the feedback variable. Again operation at 50 Hz. is assumed. As noted previously, the open loop system poles are in the right half plane for heavy loads. However, the system zeros remain in the left half plane over the full range of operating conditions. Loop closure is now practical and system stability can be maintained for motoring loads. Fig. 12 indicates the resulting pole-zero locations when the transfer function $\Delta(\sin\theta)_{eq.}/\Delta\omega_{s\ell}$ has been closed through a feedback gain G_θ = 10. The poles and zeros in the subsequent outer loop $\Delta T_e/\Delta(\sin\theta)$* are shown. It is evident that system stability has been provided by the inner feedback loop and closure of the torque regulating loop can now proceed without difficulty. Although rated line frequency has been assumed throughout this discussion, it can be shown that the system poles and zeros are not materially affected by operating frequency[3] so that these conclusions are valid over a wide speed range.

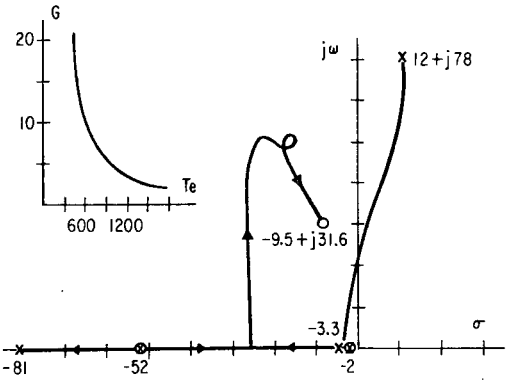

Fig. 11 Poles(x),zeros(0), and DC gain(G) of transfer function $\Delta(\sin\theta)_{eq}/\Delta\omega_{s\ell}$ with constant DC link voltage. Effect of increasing load torque with rated terminal voltage and frequency. Initial point T_e=0, final point T_e=1675 ft.lb.

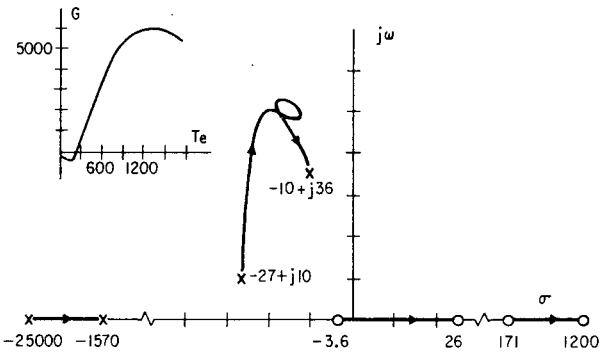

Fig. 12 Poles(x), zeros(0), and DC gain(G) of transfer function $\Delta T_e/\Delta(\sin\theta)$* Angle loop closed through gain G = 10. Initial point T_e=25, final point T_e= 1675 ft.lb.

Experimental Results

Figure 13 depicts the overall method of torque angle calculation and regulation which has been successfully implemented. This scheme consists of calculating electromagnetic torque which is then normalized by magnitude of current and magnitude of flux linkage. The intermediate signals of torque, flux magnitude, and current magnitude are already required for used in other control loops which set the desired operating points for the motor[9] so that additional sensors are not required. In order to obtain a meaningful angle signal at start-up or under abnormal operating conditions, the values of $|\hat{i}_s|$ and $|\hat{\psi}_m|$ are fed to two dividers which have a minimum value set by a non-linear limiter so that division by zero is avoided.

An alternative approach to the angle calculation which is somewhat restrictive in that saturation is not properly taken into account is shown in Fig. 14. In this case, the flux and current signals are amplified, limited and then connected to multipliers. The result is an angle signal which is not dependent on the magnitude of flux and current but only on their relative phase. For small amplitudes of current or flux, the calculation will properly yield a zero output. Division is not required. This method should lend itself well to digital implementation, although near zero speed continuous information will not be available from the digital phase detection circuit.

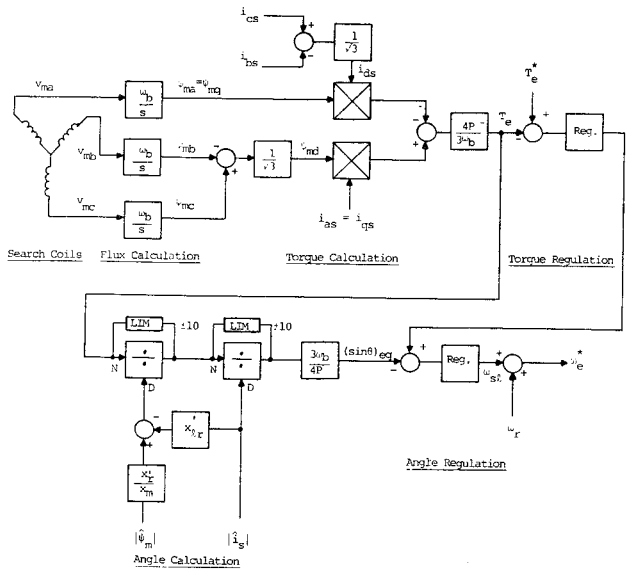

Fig. 13 Torque regulation scheme employing angle regulation.

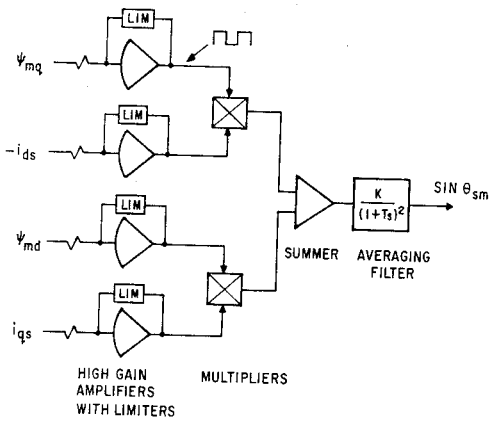

Fig. 14 Alternate Angle Computation.

The control system which has been described has been thoroughly instrumented and tested. Figure 15 shows a representative system transient response for a step change in commanded angle while operating in the motoring mode. The system parameters are again those summarized in the Appendix except that L_f = 1.0 mh. The DC source consists of a conventional six pulse rectifier bridge supplied by fixed AC voltages. The chart traces display current magnitude, torque, $(\sin\theta)_{eq}$. and motor slip frequency. It can be noted that the angle follows the command very quickly (rise time ≃ 0.04 s.) but it takes about 0.1 s. for the torque and current to respond. The slow drift in torque (about 1.0 s. time constant) is due to the change in the speed of the DC load motor as the torque level changes. The lower frequency ripple in the current is due to the beat between motor frequency and the rectifier AC source frequency. The high frequency ripple is due to the pulsations in link current caused by inverter commutation. These results clearly show that accurate, fast torque control can be achieved with synchronous control. Moreover, operation without current loop stabilization is entirely feasible.

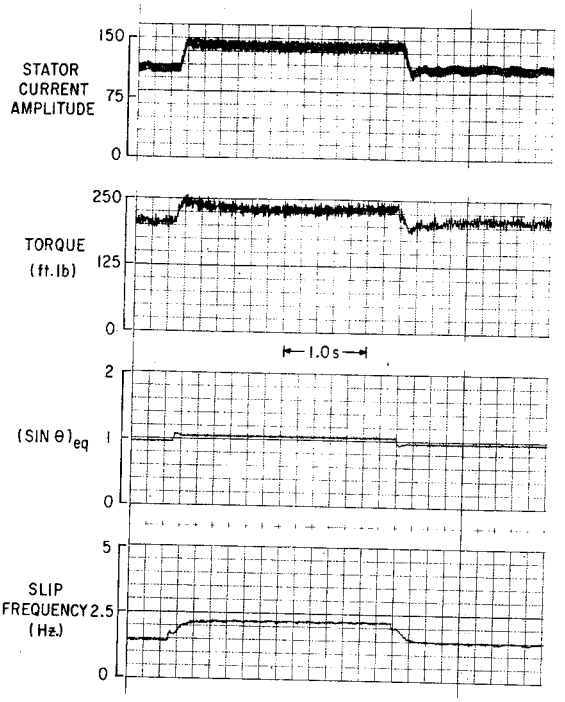

Fig. 15 Performance of prototype system for step changes in angle command with fixed DC source voltage.

Conclusion

The regulation of the angle between motor flux and current offers several direct benefits when an induction motor is supplied from a static converter. Most important, the necessary stabilizing force is exerted by inverter frequency alone, thus easing the requirements on the converter supply. Overall system stability and transient response has been shown to be enhanced by synchronous control. Moreover, the synchronization of inverter firing pulses to motor flux eliminates possible abnormal inverter commutation conditions. Problems involved with motor speed reversal with either current or voltage inverters is greatly reduced due to the vector alignment capability of the control. If necessary, mechanical sensing of shaft speed can be eliminated by controlling torque angle since the system is self-synchronous. The basic control scheme should also be beneficial to synchronous motor drives since the control scheme which has been described does not require rotor position sensing nor armature reaction compensation.

References

1. T.A. Lipo and E.P. Cornell,"State variable steady-state analysis of a controlled current induction motor drive." IEEE Trans. Industry Applications, vol. IA-11, pp. 704-712, Nov./Dec. 1975.

2. R.B. Maag,"Characteristics and application of current source/slip regulated AC induction motor drives." IEEE/IAS Annual Meeting Conference Record, pp. 411-417, Oct. 18-21, 1971.

3. T.A. Lipo and E.P. Cornell,"Modeling and design of controlled current induction motor drive systems." IEEE/IAS Annual Meeting Conference Record, pp. 612-620, Sept. 28-Oct. 2, 1975.

4. A. Abbondanti and M.B.J. Brennen,"Control of induction motor drives by synthesis of a slip signal." IEEE/IAS Annual Meeting Conference Record, pp. 845-850, Oct. 7-10, 1974.

5. G.R. Slemon, J.B. Forsythe and S.B. Dewan,"Controlled power angle synchronous motor inverter drive system." IEEE Trans. Industry Applications, vol. IA-8, pp. 679-683, Nov./Dec. 1973.

6. N. Ramesh and S.D.T. Robertson,"Induction machine instability predictions - based on equivalent circuits." IEEE Trans. Power Apparatus and Systems, vol. PAS-92, pp. 801-807, March/April 1973.

7. P.C. Krause and C.H. Thomas,"Simulation of symmetrical induction machinery." IEEE Trans. Power Apparatus and Systems, vol. PAS-84, pp. 1038-1053, Nov. 1965.

8. F. Blaschke,"The method of field orientation for the control of induction machines." Siemens Forsch. u. Entwick., pp. 184-193, Jan. 1972,(In German).

9. A.B. Plunkett,"Direct flux and torque regulation in a PWM inverter-induction motor drive." IEEE/IAS Annual Meeting Conference Record, pp. 591-597, Sept. 28-Oct. 2, 1975.

10. K.P. Kovacs and I. Racz,"Transient behavior of AC machines",(book). Hungarian Academy of Science, Budapest 1959,(in German).

11. T.A. Lipo and A.B. Plunkett,"A novel approach to induction motor transfer functions." IEEE Trans. Power Apparatus and Systems, vol. PAS-93, pp. 1410-1418, Sept./Oct. 1974.

Appendix

Motor Rating:

Rated Voltage: 210 V. RMS ℓ-n
Rated Frequency: 50 Hz.
Breakdown Torque: 1675 ft.lb.
Poles: 4

Motor Parameters at 50 Hz.

$r_s = 0.0172\ \Omega$

$x_{\ell s} = 0.0706\ \Omega$

$r'_r = 0.0310\ \Omega$

$x'_{\ell r} = 0.0903\ \Omega$

$x_m = 2.8413\ \Omega$

DC Link Parameters

$L_f = 1.824$ mh

$r_f = 0.055\ \Omega$